Theory of Line-Source Radiation from a Metal-Strip Grating Dielectric-Slab Structure

Hung-Yu David Yang, *Fellow, IEEE,* and David R. Jackson, *Fellow, IEEE*

***Abstract*—This paper describes the fundamental theory of line-source radiation from a source on a dielectric slab backed by a metal-strip grating. A continuous phased-array (CPA) method is applied to treat the analytic and numerical problems of antenna interaction with periodic structures. Both TE and TM mode cases for a one-dimensional strip grating are investigated. It is found that the strip grating on the dielectric surface may result in surface wave elimination and may also be used to support leaky waves. It is shown that high-efficiency and high-gain antennas on a dielectric substrate are possible with such metal-strip gratings.**

***Index Terms*—Dielectric slabs, gratings, Green's functions.**

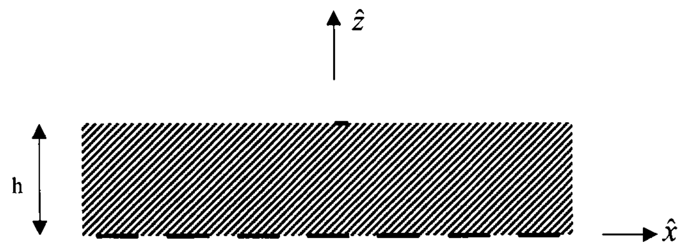

Fig. 1. Geometry of line-source radiation from a dielectric slab with metal-strip gratings.

I. Introduction

METAL-STRIP gratings on a dielectric surface have many important applications, such as frequency selective surfaces [1]–[5], leaky wave antennas [6]–[8], and wave polarizers in quasi-optical power combining [9]–[11]. A common technique for analyzing wave interaction with periodic structures is the moment-method integral-equation technique in conjunction with the Floquet theorem [1]–[5]. This method can analyze both plane-wave scattering from and guided-wave (leaky-wave) propagation on a dielectric strip-grating structure.

Radiation and scattering from antennas or objects on a strip-grating dielectric structure has much theoretical and practical interest. In printed circuit and antenna structures, microstrip elements are printed on the surface of a slab with a metal ground plane on the opposite surface. There are tremendous microwave and millimeter wave applications of such structures. However, there are several inherent disadvantages of printed circuit structures. For example, antenna gain and bandwidth are usually small and radiation efficiency is limited by the generation of surface-wave modes. However, it is known that leaky-waves, which usually result in high antenna gain and directivity, may exist in a dielectric-slab strip-grating structure. Furthermore, due to the periodic nature of the strip grating, there may exist frequency bands where surface wave can be eliminated. It is therefore conceivable that many of the disadvantages of printed circuit structures can be overcome with the use of a strip grating on the surface of the ground plane (or a two-dimensional (2-D) periodic grating on the ground plane, which is an extension of the present work).

Manuscript received July 21, 1998; revised January 14, 2000. This work was supported in part by the National Science Foundation under Grant NSF ECE 96-14469.

H.-Y. D. Yang is with the Department of Electrical Engineering and Computer Science, University of Illinois at Chicago, Chicago IL 60607 USA.

D. R. Jackson is with the Department of Electrical and Computer Engineering, University of Houston, Houston, TX 77204-4793 USA.

Publisher Item Identifier S 0018-926X(00)03269-5.

A single printed antenna on a periodic strip-grating structure is classified as an aperiodic structure, where conventional periodic moment method techniques cannot be applied directly. In such aperiodic structures, the geometry is almost periodic except for localized radiators or scatterers. A general approach to treat such aperiodic problems has been outlined and applied specifically for waveguide phased-array applications in [12]–[14]. A similar approach using a Fourier transform technique for the Green's function of a strip-grating structure was discussed in [15]. In this approach, the aperiodic structure is treated as continuous superposition of phased array structures. We refer to this scheme as a continuous phased-array (CPA) method. This unified approach, which treats the interaction of continuous and discrete plane-wave spectrums, has not received much attention.

As an initiation of the research in this direction, this paper discusses a 2-D problem of a uniform line source on the surface of a dielectric slab with an infinitely long metal-strip grating on the opposite side. The solution to this problem is essentially the Green's function for a dielectric strip-grating structure. The line source is regarded as a strip of finite width t for convenience. A longitudinal strip current corresponds to the TE mode case while a line source with a transverse strip current corresponds to the TM case. A numerically exact solution of the boundary value problem allows for the investigation of the fundamental effects of the strip grating on the antenna radiation characteristics and the understanding of the radiated, surface-wave, and leaky-wave power distributions.

II. Theory of a Line Source on a Dielectric Strip-Grating Structure

The cross section of the structure is shown in Fig. 1. The line source is a strip (width t) with current in either the $\hat{x}$ (TM) or $\hat{y}$ (TE) direction. The period of the strip grating is a and the width of the perfectly conducting metallic grating strips is w. The material dielectric constant is ε_r and the thickness of the slab is

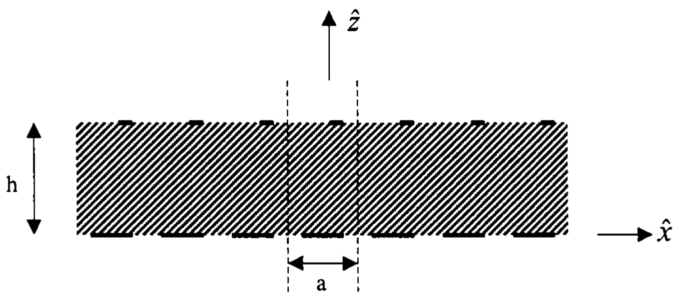

Fig. 2. Infinite phased array of line sources with metal-strip gratings. A unit cell is within $-a/2 \le x \le a/2$.

h. The line source and the center of the closest strip are offset by the distance s. Numerically exact solutions of the pertinent problem cannot be formulated directly using periodic moment methods. Therefore, instead of solving the problem directly, we first consider the geometry of an infinite phased array of line sources on the dielectric surface with the same strip grating on the opposite side, as shown in Fig. 2. The periods of the two infinite arrays (line sources and metallic strips) are the same. A progressive phase shift between the unit cells is assumed, and denoted as ϕ_x. This fictitious phased-array problem can be solved with a standard periodic moment method integral-equation approach. In particular, with the use of the Floquet (or Bloch) theorem and periodic boundary conditions, the problem is simplified to the modeling of the fields and currents within a unit cell $(-a/2 \le x \le a/2)$. Within each unit cell, there is a single line source and a metal strip. By integrating over the phase-shift variable ϕ_x, the solution of this periodic phased-array problem can be used to construct the solution to the original aperiodic (single line source) problem, as explained in more detail later. The solutions to the TM and TE cases will be considered separately below.

A. TM Case

For the TM case, the current on the line source strip and also on the strip grating is in the $\hat{x}$ direction and only E_x, E_z, and H_y components exist. As mentioned, the boundary value problem in Fig. 2 (phased-array problem) is first solved and this solution is then converted into the solution for the aperiodic structure in Fig. 1.

The TM line-source current is assumed to be piecewise sinusoidal function (with zero current at the strip edge) and the periodic strip currents on the grating are to be found. The relevant electric field integral equation (EFIE) that is enforced on the bottom strip in a unit cell is

$$E_x^{(i)}(x) + \int_{-w/2}^{w/2} G_{xx}(x-x')J_x(x')\,dx' = 0, \quad -w/2 \le x \le w/2 \tag{1}$$

where $E_x^{(i)}$ is the electric field at the bottom strip in the zero unit cell due to the top line source in the absence of the strip grating. In the method of moments, the strip current J_x is expanded in terms of several piecewise sinusoidal basis functions J_n and a Galerkin's procedure is applied to (1) to obtain the linear matrix equation

$$\sum_{n'} a_{n'} \left\langle J_n,\, \int_{-w/2}^{w/2} G_{xx}(x-x')J_{n'}(x')\,dx' \right\rangle = -\left\langle J_n,\, E_x^{(i)} \right\rangle, \qquad n = 1, 2, 3 \cdots N. \tag{2}$$

Using the expression for the Green's function for a planar slab [3], [5] (without the grating strips), it can be shown that the inner product of the line-source (primary) electric field and the nth testing (weighting) piecewise sinusoidal function (on the strip grating in the unit cell) is

$$\left\langle J_n,\, E_x^{(i)} \right\rangle = \frac{1}{2j\omega\varepsilon_0\varepsilon_r a} \sum_{m=-\infty}^{\infty} \left[e^{-q_1 h} + 2\,\frac{\cosh q_1 h + \alpha e^{q_1 h}}{\alpha^2 e^{2q_1 h} - 1} \right] \cdot q_1 f_1 f_2 e^{-jk_{xm}\Delta_n} \tag{3}$$

where $\Delta_n = -w/2 + nw/(N+1) - s\Delta_n$ with N the number of expansion functions

$$\alpha = \frac{\varepsilon_r q_0 + q_1}{\varepsilon_r q_0 - q_1} \tag{4}$$

$$q_1 = \sqrt{k_{xm}^2 - k_0^2 \varepsilon_r} \tag{5}$$

$$q_0 = \sqrt{k_{xm}^2 - k_0^2} \tag{6}$$

and $k_{xm} = (2m\pi/a) + (\phi_x/a)$. Also, f_1 and f_2 are the Fourier transform of the piecewise sinusoidal functions for the line-source and the strip-grating currents, respectively, given as

$$f_1 = \frac{2k_e}{\sin(k_e t/2)}\,\frac{\cos(k_e t/2) - \cos(k_{xm} t/2)}{k_{xm}^2 - k_e^2} \tag{7}$$

$$f_2 = \frac{2k_e}{\sin(k_e\, d)}\,\frac{\cos(k_e d) - \cos(k_{xm}\, d)}{k_{xm}^2 - k_e^2} \tag{8}$$

where $d = w/(N+1)$ and $k_e = k_0\sqrt{(\varepsilon_r + 1)/2}$ is the effective wavenumber for the currents on the strips, chosen to best simulate the actual current distribution for narrow strips. In addition, the self reaction of the strip-grating basis functions is

$$\left\langle J_n,\, \int G_{xx} J_{n'}\,dx' \right\rangle = \frac{1}{2j\omega\varepsilon_0\varepsilon_r a} \sum_{m=-\infty}^{\infty} \left[1 + 2\,\frac{1 + \alpha_e^{q_1 h}\cosh q_1 h}{\alpha^2 e^{2q_1 h} - 1} \right] \cdot q_1 f_2^2 e^{-jk_{xm}\Delta_{nn'}} \tag{9}$$

where $\Delta_{nn'} = d(n - n')$. Equation (9) is obtained again using the Green's function for the grating strips on a planar slab [3]. The solution of the linear matrix equation in (2) provides the current distribution on the grating strip in the zero unit cell. Once the currents on the grating are known, the fields from the grating currents may be determined and added to the field of the periodic line-source excitation to find the total field of the phased-array problem. Omitting the details, the field E_x for the phased-array problem can be written in the following form:

$$E_x^p(x, z; \phi_x) = \frac{1}{a} \sum_{m=-\infty}^{\infty} \overline{E}_{xm}^p(z; \phi_x) e^{-jk_{xm}x}. \qquad (10)$$

The solution for E_x in the structure shown in Fig. 1 can be found from (10) through the following equation:

$$E_x(x, z) = \frac{1}{2\pi} \int_{-\pi}^{\pi} \overline{E}_x^p(x, z; \phi_x)\, d\phi_x. \qquad (11)$$

The integration in (11) represents a superposition of the solutions to the periodic phased-array problem. The key is the superposition principle and phase cancellation. When we perform the integration in (11), we are in effect cancelling out all other line sources except the one with zero phase angle, in the zero unit cell. Using the summation form in (10), (11) can be written in a form similar to that for radiation from a line source in the absence of the grating, namely

$$E_x(x, z) = \frac{1}{2\pi} \int_{-\infty}^{\infty} \tilde{E}_x(k_x, z)\, e^{-jk_x x}\, dk_x. \qquad (12)$$

This can be obtained by starting with

$$E_x(x, z) = \frac{1}{2\pi a} \int_{-\pi}^{\pi} \sum_{m=-\infty}^{\infty} \overline{E}_{xm}^p(z; \phi_x)\, e^{-jk_{xm}x}\, d\phi_x \qquad (13)$$

and then using the property that

$$\overline{E}_{xm}^p(z; \phi_x) = \overline{E}_{x0}^p(z; \phi_x + 2\pi m).$$

It is then seen that

$$\tilde{E}_x(k_x, z) = \frac{1}{a} \overline{E}_{x0}^p(z; \phi_x).$$

Similarly, the magnetic field in the structure can be written according to (13) as

$$H_y(x, z) = \frac{1}{2\pi a} \int_{-\pi}^{\pi} \sum_{m=-\infty}^{\infty} \overline{H}_{ym}^p(z; \phi_x)\, e^{-jk_{xm}x}\, d\phi_x. \qquad (14)$$

The magnetic field in (14) is due to both the line-source current and the strip-grating currents.

In this work, the quantities of interest are the radiated power, surface-wave power, and the associated parameters. If the structure were assumed lossless, the radiated power and surface-wave power would determine the radiation efficiency of the line source. Equation (14) describes the magnetic field in the structure shown in Fig. 1. Radiated far-zone fields are found from (14) by using the method of steepest descent [16]. The saddle point is at $k_x = k_0 \sin\theta$ ($\phi_x = k_0 a \sin\theta$) for the upper-space radiation, where θ is the angle measured from the z-axis (Fig. 1). Normally, the saddle point will only be encountered in the $m = 0$ Floquet mode term, assuming only one propagating mode. As a result, the far-zone magnetic field in the upper space region $z > h$ is

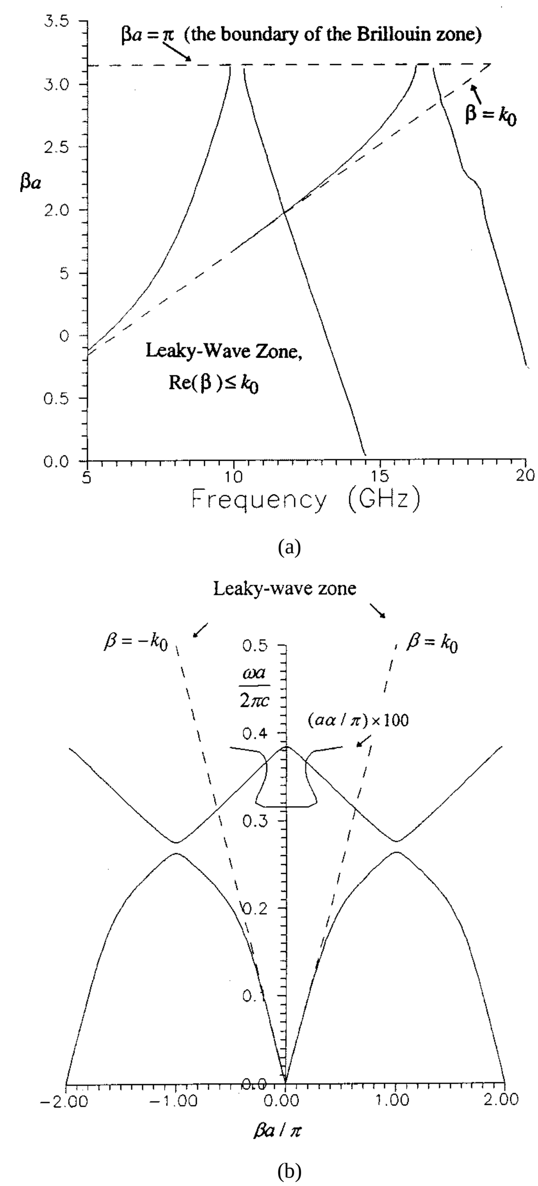

Fig. 3. TM surface-wave and leaky-wave mode diagram for a dielectric strip-grating structure: $\varepsilon_r = 10$, $h = 5$ mm, $w = 2$ mm, $s = 0$, and $a = 8$ mm.

$$H_y^{(}R, \theta) = \sqrt{\frac{k_0}{2\pi R}}\, \cos\theta \overline{H}_{y0}^p(\theta)\, e^{-jk_0 R + j(\pi/4)} \qquad (15)$$

where $\overline{H}_{y0}^p(\theta)$ is the term in (14) with $m = 0$ and $\phi_x = k_0 a \sin\theta$. The far-zone average radiated power density is $(\eta_0/2)|H_y(R, \theta)|^2$ and the total radiated power per unit length (in the y direction) in the upper space region is

$$P_{rad} = \int_{-\pi/2}^{\pi/2} \frac{\eta_0}{2}\, |H_y(R, \theta)|^2\, R\, d\theta. \qquad (16)$$

The saddle-point method can also be applied to calculate the radiation in the lower-space region $(z < 0)$ in a similar way as described in connection with (15) and (16).

The surface-wave fields are found from (14) by using a pole-residue technique [17]. The surface-wave magnetic field is written as

$$\begin{aligned} H_y^{sw}(x, z) &= \frac{-j}{a} \sum_i \sum_{m=-\infty}^{\infty} \mathrm{Res}\left[\overline{H}_{ym}^p(z, \phi_x) e^{-jk_{xm}^x}\right]_{\phi_x=\phi_{sw}^i} \\ &\quad \text{if } x \gg 0 \\ &= \frac{j}{a} \sum_i \sum_{m=-\infty}^{\infty} \mathrm{Res}\left[\overline{H}_{ym}^p(z, \phi_x) e^{-jk_{xm}x}\right]_{\phi_x=-\phi_{sw}^i} \\ &\quad \text{if } x \ll 0 \end{aligned} \tag{17}$$

where ϕ_{sw}^i is the surface-wave pole. Note that the far-zone surface waves propagate on a periodic structure and are in an infinite summation form (infinite number of Floquet modes associated with each surface wave mode). The energy-transport velocity for a surface-wave mode is equal to the group velocity [18] and, hence, total surface wave power P_{sw}per unit length in the y direction is

$$P_{sw} = \sum_{p=1}^{P} \frac{1}{a\,|d\beta_p/d\omega|} \left(W_e^{(p)} + W_m^{(p)}\right) \tag{18}$$

where β_p is the propagation constant for the pth surface wave mode and the energy stored in a unit cell is

$$W_e^{(p)} + W_m^{(p)} = 2W_m^{(p)} = \int_{-\infty}^{\infty} \int_0^a \frac{\mu}{2} |H_y^{sw}|^2 \, dx \, dz. \tag{19}$$

The above integrations can be performed analytically, although the details are omitted here.

B. TE Case

For the TE case, the strip current is in the $\hat{y}$ direction (Fig. 1) and only H_x, H_z, and E_y components exist. Similar to the TM mode case, we first solve the boundary value problem shown in Fig. 2 and convert the solution to that for the aperiodic structure shown in Fig. 1. The line-source current for the TE case is taken as a pulse function over the width t (an approximation that allows for a nonzero edge-current). The EFIE for the metallic strip in the zero unit cell is

$$\begin{aligned} E_y^{(i)}(x) &+ \int_{-w/2}^{w/2} G_{yy}(x-x') J_y(x')\, dx' \\ &= 0, \qquad -w/2 \le x \le w/2 \end{aligned} \tag{20}$$

where $E_y^{(i)}$ is the electric field at the bottom strip due to the top line source in the absence of the strip grating. In the method of moments, the strip-grating current J_y is expanded in terms of several pulse functions j_n (since J_y is nonzero at the strip edge, pulse-expansion functions are more appropriate than sinusoidal functions) and a Galerkin's procedure is applied to obtain a linear matrix equation

$$\begin{aligned} \sum_{n'} a_{n'} &\left\langle J_n, \int_{-w/2}^{w/2} G_{yy}(x-x') J_{n'}(x')\, dx' \right\rangle \\ &= -\left\langle J_n, E_y^{(i)} \right\rangle, \qquad n = 1, 2, 3 \cdots N. \end{aligned} \tag{21}$$

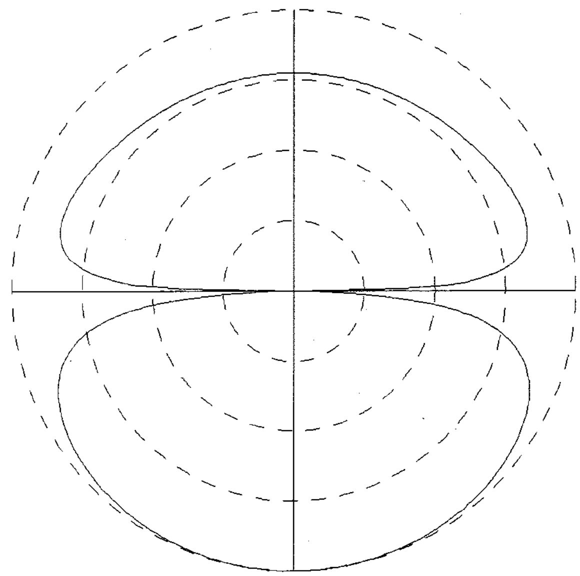

Fig. 4. Radiation patterns of a TM line source radiating from a dielectric strip grating structure: $F = 5$ GHz and all other parameters are described in Fig. 3.

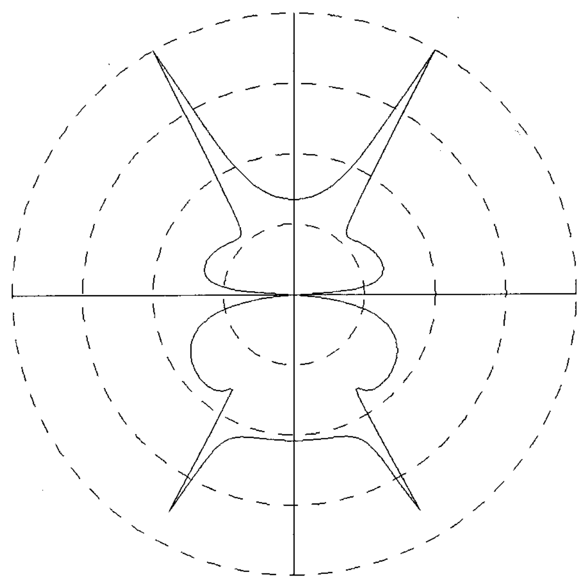

Fig. 5. Radiation patterns of a TM line source radiating from a dielectric strip grating structure: $F = 13$ GHz and all other parameters are described in Fig. 3.

Similar to the TM case, it can be shown from the Green's function for a dielectric slab that

$$\begin{aligned} &\left\langle j_n, E_y^{(i)} \right\rangle \\ &= \frac{-j\omega\mu_0}{2a} \sum_{m=-\infty}^{\infty} \left[e^{-q_1 h} + 2\,\frac{\cosh q_1 h - \gamma e^{q_1 h}}{\gamma^2 e^{2q_1 h} - 1}\right] \\ &\quad \cdot \frac{g_1 g_2}{q_1}\, e^{-jk_{xm}\Delta_n} \end{aligned} \tag{22}$$

where $\Delta_n = -w/2 + nw/(N+1) - s$ with N the number of expansion functions and

$$\gamma = \frac{q_0 + q_1}{q_0 - q_1}. \tag{23}$$

Also, g_1 and g_2 are the Fourier transforms of the pulse functions for the line source and the strip grating, respectively, given as

$$g_1 = \frac{\sin(k_{xm}t/2)}{k_{xm}t/2} \tag{24}$$

$$g_2 = \frac{\sin(k_{xm}\, d)}{k_{xm}\, d}. \tag{25}$$

In addition, the self reaction of the pulse-basis functions can be expressed as

$$\left\langle j_n,\, \int_{-w/2}^{w/2} G_{yy} j_{n'}\, dx \right\rangle = \frac{-j\omega\mu_0}{2a} \sum_{m=-\infty}^{\infty} \left[1 + 2\,\frac{1-\gamma_e^{q_1 h}\cosh q_1 h}{\gamma^2 e^{2q_1 h} - 1}\right] \cdot \frac{g_2^2}{q_1}\, e^{-jk_{xm}\Delta_{nn'}} \tag{26}$$

where $\Delta_{nn'} = d(n-n')$ and d is the width of the pulse functions on the grating strips. The solution for the field component E_y of the phased-array problem due to both the line source and grating strips can be written in the following form similar to that for the TM case as:

$$E_y^p(x,\, z;\, \phi_x) = \frac{1}{a} \sum_{m=-\infty}^{\infty} \overline{E}_{ym}^p(z;\, \phi_x) e^{-jk_{xm}x}. \tag{27}$$

The solution for E_y in the structure shown in Fig. 1 can be found from (27) by integrating over the interelement phase-shift variable as before. The E_y component for the TE case is then written as

$$E_y(x,\, z) = \frac{1}{2\pi_a} \int_{-\pi}^{\pi} \sum_{m=-\infty}^{\infty} \overline{E}_{ym}^p(z;\, \phi_x) e^{-jk_{xm}x}\, d\phi_x. \tag{28}$$

Similar to the TM case, a saddle point exists at $k_x = k_0 \sin\theta$ ($\phi_x = k_0 a \sin\theta$), and the far-zone electric field in the upper-space region $z > h$ is then

$$E_y(R,\, \theta) = -j\omega\mu_0 \sqrt{\frac{k_0}{2\pi R}} \cos\theta \overline{E}_{y0}^p(\theta) e^{-jk_0 R + j(\pi/4)} \tag{29}$$

where $\overline{E}_{y0}^p(\theta)$ is the term in (28) with $m = 0$ and $\phi_x = k_0 a \sin\theta$. The far-zone average radiated power density per unit length is $|E_y(R,\, \theta)|^2/(2\eta_0)$ and the total radiated power per wavelength (in the y direction) in the upper-space region is

$$P_{rad} = \frac{1}{2\eta_0} \int_{-\pi/2}^{\pi/2} |E_y(R,\, \theta)|^2\, R\, d\theta. \tag{30}$$

The far-zone surface-wave fields are found from (28) from the pole residue. The surface-wave magnetic field is written as

$$E_y^{sw}(x,\, z) = \frac{-j}{a} \sum_i \sum_{m=-\infty}^{\infty} \text{Res}\left[\overline{E}_{ym}^p(z;\, \phi_x) e^{-jk_{xm}^x}\right]_{\phi_x = \phi_{sw}^i} \quad \text{if } x \gg 0$$

$$= \frac{j}{a} \sum_i \sum_{m=-\infty}^{\infty} \text{Res}\left[\overline{E}_{ym}^p(z;\, \phi_x) e^{-jk_{xm}x}\right]_{\phi_x = -\phi_{sw}^i} \quad \text{if } x \ll 0. \tag{31}$$

The total surface wave power P_{sw} is given by the same formula as the TM formula (18) except that it is now more convenient to express the stored energy in the unit cell as

$$W_e^{(p)} + W_m^{(p)} = 2W_e^{(p)} = \int_{-\infty}^{\infty} \int_0^a \frac{\varepsilon}{2} |E_y^{sw}|^2\, dx\, dz. \tag{32}$$

III. Results and Discussions

The validity of the present analysis has been justified by comparisons with several limiting cases where results are known. For example, when the line source is placed within the grating and the slab dielectric constant is set to one, identical field patterns in the upper and lower space are found. When the strip width is close to the grating period (to simulate a ground plane), the results approach those for the case of a grounded slab structure. The leaky-wave beam angle is also validated by comparing to the phase constant (real part of the complex wavenumber) for the leaky mode on the structure.

A printed antenna on a grounded dielectric-slab structure usually has a low gain and the radiation efficiency is limited by surface wave losses. The strip grating on the back of the dielectric slab can significantly affect the radiation characteristics. An example of the mode diagram for TM guided waves excited by a TM line source is first shown in Fig. 3. At low frequencies, the guided-wave mode is a perturbation of the surface wave mode without the grating. When βa approaches π, the guided-wave propagation constant become complex valued and the solution appears as a complex-conjugate pair. The modes in this region, where $\beta a = \pi$, are nonpropagating modes (evanescent), where the attenuation corresponds to reactive decay and not radiation. In periodic waveguides, the frequency range where the modes are complex modes is often called the propagation (or photonic) bandgap [18]. Within the bandgap zone surface-wave propagation is eliminated, which may result a significant increase in antenna radiation efficiency. The line $\beta a = \pi$ in Fig. 3(a) is also the boundary of the Brillouin irreducible zone. Due to the periodic nature of the structure, if βa is above the boundary of this zone (there are infinite number of such values), there is a corresponding βa below the boundary (within the Brillouin zone) that represents the same mode. As the frequency increases beyond the stopband region, the wavenumber once again becomes pure real, corresponding to a propagating mode.

As frequency further still increases, the phase constant eventually crosses below the $\beta = k_0$ line and the propagation wavenumber becomes complex-valued due to radiation. In this case, the guide-wave mode becomes a fast (physically meaningful) leaky-wave mode. When the phase constant is less than the free-space wave number, as seen from (6), there exists a Floquet mode (usually the $m = -1$ mode) such that q_0 is no longer real and positive. In the leaky-mode region the real part of q_0 is negative and the imaginary part is positive. Because the wave propagates as $\exp(-q_0|z|)$ away from the structure, there is energy propagating into the upper or lower space and

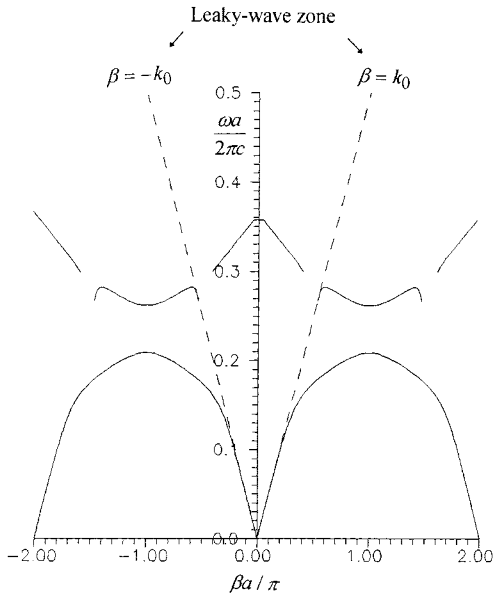

Fig. 6. TM surface-wave and leaky-wave mode diagram for a dielectric strip-grating structure: $\varepsilon_r = 10$, $h = 5$ mm, $w = 6$ mm, $s = 0$, and $a = 8$ mm.

the guided surface wave becomes leaky, with an exponential increase transversely from the structure. It is seen from Fig. 3(a) that the surface-wave bandgap and the leaky-wave phenomenon are found for not only the fundamental mode, but also the higher order modes (i.e., higher order slab modes that are perturbed by the grating). It is noted that when the frequency is high enough such that $0.5 \leq a/\lambda_0$, all the propagating surface wave modes turn into leaky wave modes (there is always an m such that q_0 is a complex value). Fig. 3(b) shows the same $\omega - \beta$ diagram for the fundamental mode but in a more customary way for a periodic structure [18], [19]. The stopband region is clearly seen as the "gap" that occurs at $\beta a = \pi$.

A typical radiation pattern of a TM line source on a dielectric strip grating structure without leaky-wave excitation is shown in Fig. 4. The parameters are the same as for the results in Fig. 3 and the frequency is at 5 GHz. As is expected, the antenna gain is low with a null on the horizon. It is interesting to observe that there is about 10-dB higher gain for the main beam in the lower space than the one in the upper space. This implies that most of the power is radiating into the lower space. In other words, the strip grating acts more like a director than a reflector.

The excitation of leaky waves may greatly enhance the antenna gain (directivity). An example of such a radiation pattern is shown in Fig. 5. The results are for the case in Fig. 3 again but at 13 GHz, where there is a leaky wave radiating at beam angle $\theta \approx 30°$. It is seen that due to the excitation of a leaky wave the antenna pattern is highly directive. Such a high-gain leaky-wave antenna had been experimentally demonstrated [6], [7].

It is observed from Fig. 3 that the transition from a surface wave to a leaky-wave is essentially continuous. This observation is not always true, especially when the grating strips are wide (slot width is narrow). An example is shown in Fig. 6 where the parameters are the same as those in Fig. 3 except that the grating strip width is now 6 mm. It is seen

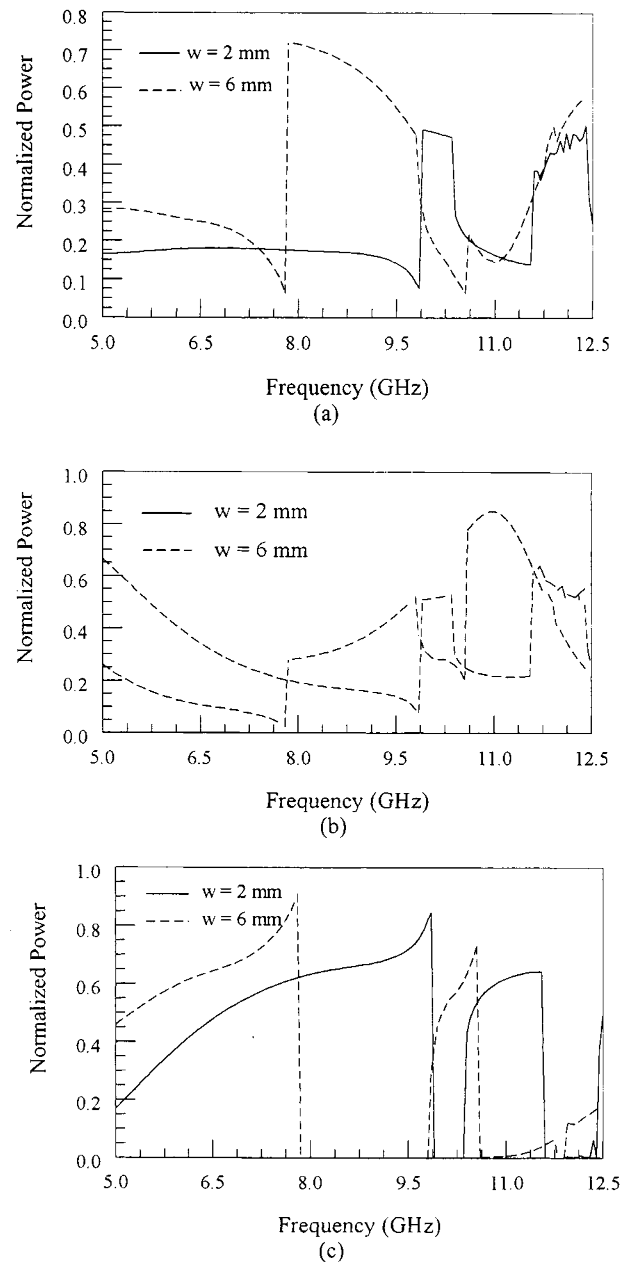

Fig. 7. Power emanating from a TM-line source on a dielectric strip-grating structure. Total power is 1 W. $\varepsilon_r = 10$, $h = 5$ mm, $w = 2$ mm, $s = 0$, $t = 1$ mm and $a = 8$ mm. (a) Power into upper space. (b) Power into lower space. (c) Power into surface waves.

that there is a mode discontinuity near the boundary of the physical leakage region.

The strip-grating structure may result in surface-wave elimination within the propagation bandgap zone. The radiation efficiency of an antenna within such a zone may be greatly enhanced. An example is shown in Fig. 7(a)–(c). The power distributions versus frequency among the radiated powers in the upper and lower spaces and the surface wave are shown. There are two cases shown in the figures, with a grating strip width of 2 mm (the mode diagram is shown in Fig. 3) and 6 mm (the mode diagram is shown

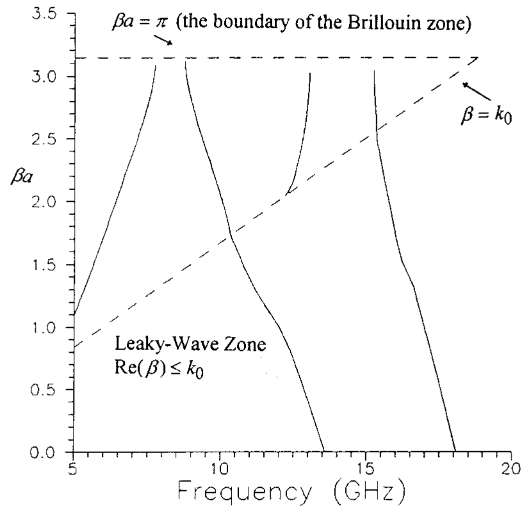

(a)

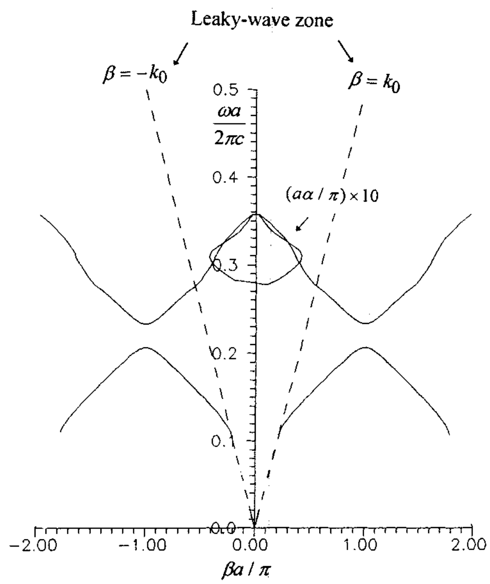

(b)

Fig. 8. TE surface-wave and leaky-wave mode diagram for a dielectric strip-grating structure: $\varepsilon_r = 10$, $h = 5$ mm, $w = 2$ mm, $s = 0$, and $a = 8$ mm.

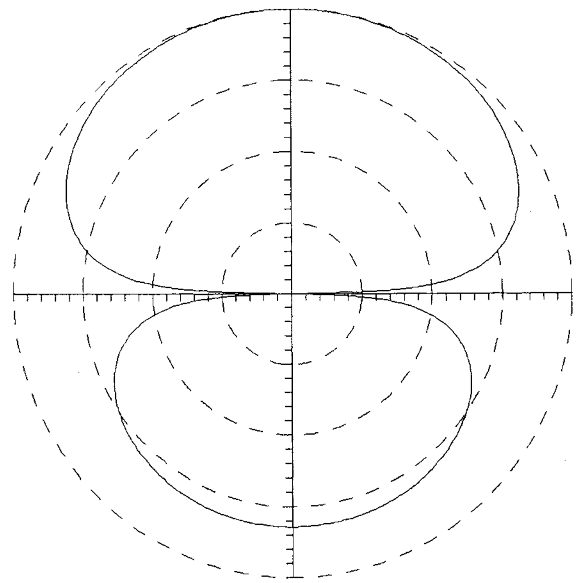

Fig. 9. Radiation patterns of a TE line source radiating from a dielectric strip grating structure: $F = 5$ GHz and all other parameters are described in Fig. 8.

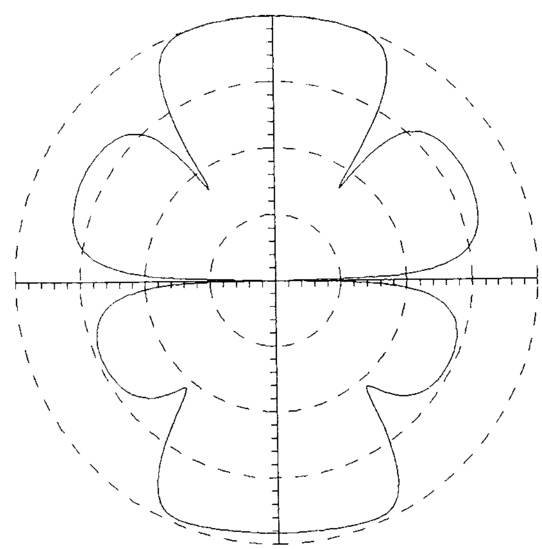

Fig. 10. Radiation patterns of a TE line source radiating from a dielectric strip grating structure: $F = 12$ GHz and all other parameters are described in Fig. 8.

in Fig. 6). The grating period is 8 mm in both cases. At very low frequencies (large wavelength), the dielectric substrate has no effect on the radiation, there is very little surface-wave power, and the radiated power is evenly divided above and below the line source. As the frequency increases, the effects of the dielectric substrate and strip grating increase, so that the upper-space radiated power decreases and the lower-space radiated power increases until minimum and maximum are reached, respectively (this occurs at a frequency lower than 5 GHz). As frequency increases further, the lower space power decreases and upper space power increases, as is observed in Fig. 7(a) and (b) and also Fig. 4. The surface-wave power increases with frequency before the bandgap zone. Within the surface-wave bandgap (without surface wave losses), it is seen that there is a dramatic increase in the percentage of power radiated into the upper and lower spaces. The surface-wave bandgap zone is very much dependent on the width of the strip grating. It is seen that wider strips result in a wider bandgap, and that the bandgap occurs at lower frequencies. The frequency at which leakage begins occurs when the phase constant is equal to free-space wave number. In the illustrated case, Fig. 7(c), this frequency is 11.58 GHz for $w = 2$ mm and is 10.4 GHz for $w = 6$ mm. At these frequencies the surface-wave power goes to zero (there is no longer a surface wave, but only a leaky wave).

Although the examples discussed so far are for the TM case (the line current is in the x direction), similar observations also hold for the TE case (line current in the y direction). An example of the mode diagram for the guided waves excited by a TE line source is shown in Fig. 8. The parameters of the dielectric strip-grating structure are the same as for the TM case in Fig. 3. It is seen that the bandgap zone occurs at lower frequencies for the TE case. This is due to the fact that the TE surface-wave mode phase constant increases with frequency more rapidly than in the TM case.

A typical radiation pattern of a TE line source on a dielectric strip-grating structure without leaky-wave excitation is shown in Fig. 9. The parameters are the same as for the results shown for the TM case (Fig. 4). It is interesting to observe that there is almost a 10-dB higher gain for the main beam in the upper space than for the one in the lower space, opposite to the TM case. This implies that most power radiates into the upper space; that is, the strip grating acts more like a reflector than a director.

An example of a leaky-wave radiation pattern for the TE case is shown in Fig. 10. The results are for the case in Fig. 9, but the frequency is at 12 GHz instead. It is seen from Fig. 10 that the directivity of the TE line source is not high as for the TM case shown in Fig. 5. In fact, sharp nulls are observed in the TE case instead of the sharp beams in the TM case. This is probably due to the fact that for this set of parameters, the leaky-wave radiation pattern is almost perfectly cancelling the "space-wave" pattern due to the rest of the continuous spectrum (representing direct radiation from the line source into space), at the beam peak.

An example of power distributions versus frequency for the powers in the upper and lower spaces and the surface wave, is shown in Fig. 11(a)–(c) for the TE case. There are two cases shown in the figures, corresponding to a grating strip width of 2 and 6 mm, with period of 8 mm in both cases. It is seen that at low frequencies, the behavior of the radiated powers in the upper and lower space versus frequency is opposite to the TM case. There are several interesting observations for the TE case. First, the surface-wave mode has a smoother transition to the bandgap zone than for the TM case. Also, inside the bandgap zone, for the small grating strip width ($w = 2$ mm), most of the radiated power is into the lower space (little into the upper space) and the grating strips therefore act somewhat transparent. For the large grating strip width ($w = 6$ mm), the opposite observation is found and the grating strips act more like a metal shield inside the band gap. The frequency at which leakage begins in Fig. 11(c) is 10.3 GHz for $w = 2$ mm and 10.2 GHz for $w = 6$ mm. Once again, the surface-wave power goes to zero at these frequencies.

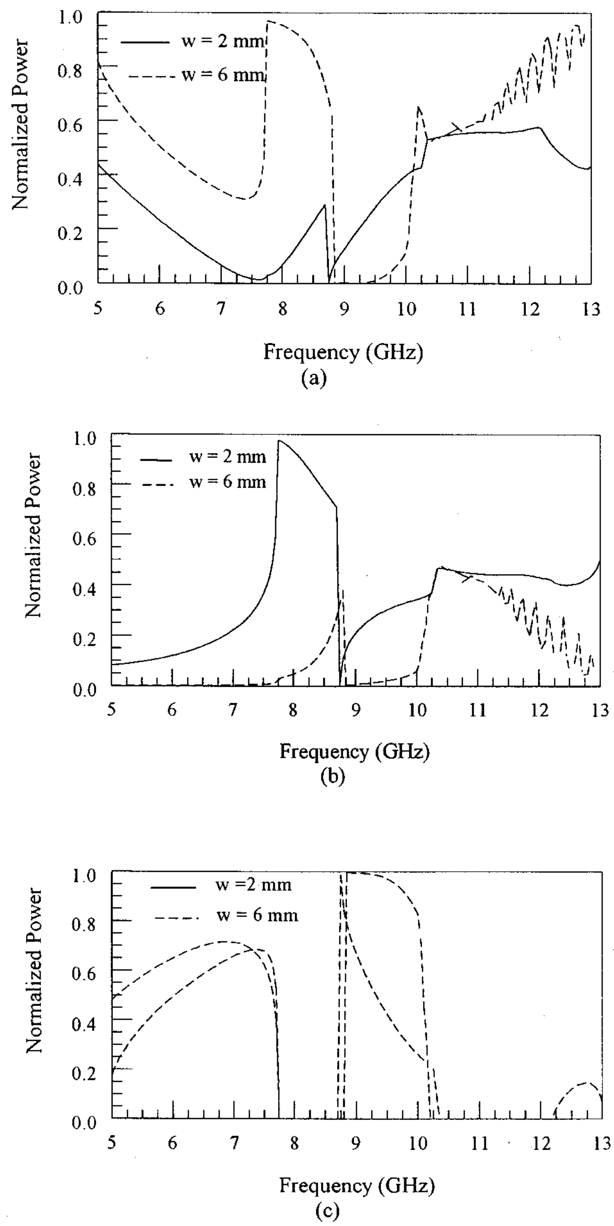

Fig. 11. Power emanating from a TE-line source on a dielectric strip-grating structure. Total power is 1 W. $\varepsilon_r = 10$, $h = 5$ mm, $w = 2$ mm, $s = 0$, $t = 1$ mm, and $a = 8$ mm. (a) Power into upper space. (b) Power into lower space. (c) Power into surface waves.

IV. Conclusions

In this paper, the theory of radiation from a line source on a dielectric slab backed by a periodic metal strip grating was described. A continuous phased-array approach was applied to solve for the fields of the corresponding aperiodic structure (single source in the presence of the periodic structure). A moment method was first applied to the periodic phased-array structure where an infinite periodic array of line source exists, with an arbitrary interelement phase shift. The superposition of the corresponding phased-array solutions over all the possible phase-shift angles (from $-\pi$ to π) results in the solution of the pertinent aperiodic structure. Both TM and TE line-source excitation problems were investigated. It was found that the strip grating affects significantly the radiation characteristics of the line source. The strip grating introduces surface-wave band gap frequency regions (surface wave elimination), resulting in significant increases in antenna radiation efficiency. The strip grating structure may also support leaky waves. It was found that the excitation of the leaky waves greatly enhances antenna gain (directivity) for the TM case but not for the TE case, when the line source is on top of the slab. Power distributions among the radiated waves and the surface waves as a function of structural parameters were also investigated. It was observed that the surface-wave bandgap zone is very much dependent on the width of the strip grating. Further problems involving planar-strip gratings on a dielectric slab using microstrip dipoles and patches as the radiating elements are presently under investigation.

REFERENCES

[1] T. K. Wu, Ed., *Frequency Selective Surfaces and Grid Arrays*. New York: Wiley, 1995.

[2] R. J. Mittra, C. H. Chan, and T. A. Cwik, "Techniques for analyzing frequency selective surfaces—A review," in *Proc. IEEE*, vol. 76, Dec. 1988, pp. 1593–1614.

[3] J. P. Montgomery, "Scattering by an infinite periodic array of thin conductors on a dielectric sheet," *IEEE Trans. Antennas Propagat.*, vol. AP-23, pp. 70–75, Jan. 1975.

[4] H. A. Kalhor, "Electromagnetic scattering by a dielectric slab loaded with a periodic array of strips over a ground plane," *IEEE Trans. Antennas Propagat.*, vol. 36, pp. 147–151, Jan. 1988.

[5] A. L. Adonina and V. P. Shestopalov, "Diffraction of electromagnetic waves obliquely incident on a plane metallic grating with a dielectric slab," *Soviet Phys.-Tech. Phys.*, vol. 8, no. 6, pp. 479–486, December 1963.

[6] A. Ip and D. R. Jackson, "A leaky-wave antenna using a two-dimensional periodic array of metal patches," in *IEEE Int. Symp. Antennas Propagat. Dig.*, Newport Beach, CA, June 1995, pp. 1652–1655.

[7] C. N. Hu and C.-K. Tzuang, "Microstrip leaky-mode antenna array," *IEEE Trans. Antennas Propagat.*, vol. 45, pp. 1698–1699, Nov. 1997.

[8] A. A. Oliner and K. S. Lee, "Microstrip leaky-wave strip antennas," in *IEEE Int. Symp. Antennas Propagat. Dig.*, Philadelphia, PA, June 1986, pp. 443–446.

[9] M. Kim, J. R. Rosebberg, R. P. Smith, R. M. Weikle, J. B. Hacker, M. P. Delisio, and D. B. Rutledge, "A grid amplifier," *IEEE Microwave Guided Wave Lett.*, vol. 1, pp. 322–324, Nov. 1991.

[10] J. W. Mink, "Quasioptical power combining of solid-state millimeter-wave sources," *IEEE Trans. Microwave Theory Tech.*, vol. MTT-34, pp. 273–279, Feb. 1986.

[11] S. C. Bundy and Z. B. Popovic, "A generalized analysis for grid oscillator design," *IEEE Trans. Microwave Theory Tech.*, vol. 42, pp. 2486–2491, Dec. 1994.

[12] S. W. Lee, "Radiation from an infinite aperiodic array of parallel-plate waveguide," *IEEE Trans. Antennas Propagat.*, vol. AP-15, pp. 598–606, Sept. 1967.

[13] V. Galindo, "A generalized approach to a solution of aperiodic arrays and modulated surfaces," *IEEE Trans. Antennas Propagat.*, vol. AP-16, pp. 424–429, July 1968.

[14] Y. T. Lo, "Random periodic arrays," *Radio Sci.*, vol. 3, no. 5, May 1968.

[15] R. A. Sigelmann and A. Ishimaru, "Radiation from aperiodic structures excited by an aperiodic source," *IEEE Trans. Antennas Propagat.*, vol. AP-13, pp. 354–364, May 1965.

[16] C. M. Bender and S. A. Orszag, *Advanced Mathematics Methods for Scientists and Engineers*. New York: McGraw-Hill, 1978, p. 279.

[17] N. G. Alexopoulos and D. R. Jackson, "Fundamental superstrate (cover) effects on printed circuit antennas," *IEEE Trans. Antennas Propagat.*, vol. AP-32, pp. 807–816, Aug. 1984.

[18] R. E. Collin, *Field Theory of Guided Waves*. New York: IEEE Press, 1991, p. 627.

[19] ——, *Foundations for Microwave Engineering*, 2nd ed. New York: McGraw-Hill, 1992, p. 565.

Hung-Yu David Yang (S'87–M'88–SM'93–F'00) received the B.S. degree in electrical engineering from the National Taiwan University, Taipei, and the M.S. and Ph.D. degrees in electrical engineering from the University of California at Los Angeles, in 1982, 1985, and 1988, respectively.

Since 1992, he has been with the Electrical Engineering and Computer Science Department, University of Illinois at Chicago, and is currently an Associate Professor. He has published more than 80 technical journal and conference papers. He has served as the Editor-in-Chief of *Electromagnetics* since 1997. His research interests include computational methods for radiation and scattering from aperiodic structures, microwave and applications of two- and three-dimensional periodic structures, millimeter-wave and quasi-optical applications of photonic bandgap materials, passive components in microwave integrated circuits, wave interaction with complex media, and printed circuits and antennas on gyrotropic media.

Dr. Yang has served as a Technical Program Committee Member of the IEEE International Microwave Symposium since 1994. He was an Associate Editor of IEEE TRANSACTIONS ON ANTENNAS AND PROPAGATION from 1995 to 1998. He is a member of URSI Commission B and Sigma Xi.

David R. Jackson (S'83–M'84–SM'95–F'99) was born in St. Louis, MO, on March 28, 1957. He received the B.S.E.E. and M.S.E.E. degrees from the University of Missouri, Columbia, in 1979 and 1981, respectively, and the Ph.D. degree in electrical engineering from the University of California, Los Angeles, in 1985.

From 1985 to 1991, he was an Assistant Professor in the Department of Electrical and Computer Engineering at the University of Houston, TX. From 1991 to 1998 he was an Associate Professor in the same department and, since 1998, he has been a Professor there. He is also presently serving as a Distinguished Lecturer for the IEEE AP-S Society. He is presently an Associate Editor for the *International Journal of RF and Microwave Computer-Aided Engineering*. He is a past associate editor of the *Journal of Radio Science*. His research interests currently include computer-aided design of microstrip antennas and circuits, microstrip antenna analysis and design, periodic structures, and (cover) effects on printed circuit antennas.

Dr. Jackson is a past Associate Editor for the IEEE TRANSACTIONS ON ANTENNAS AND PROPAGATION. He is presently serving as the Chapter Activities Coordinator for the AP-S Society of the IEEE and as the Chair of the Technical Activities Committee for URSI U.S. Commission B.